Biophysical Journal Volume 67 August 1994 793–803

Restoration of Junctional Tetrads in Dysgenic Myotubes by Dihydropyridine Receptor cDNA

H. Takekura,*‡ L. Bennett,§ T. Tanabe,¶ K. G. Beam,§ and C. Franzini-Armstrong*

*Department of Cell and Developmental Biology, University of Pennsylvania School of Medicine, Philadelphia, Pennsylvania; ‡Department of Physiology and Biomechanics, National Institute of Fitness and Sports, Kagoshima, Japan; §Department of Physiology, Colorado State University, Ft. Collins, Colorado; ¶Howard Hughes Medical Institute, Department of Cellular and Molecular Physiology, Yale University, New Haven, Connecticut USA

ABSTRACT Excitation-contraction coupling was restored in primary cultures of dysgenic myotubes by transfecting the cells with an expression plasmid encoding the rabbit skeletal muscle dihydropyridine receptor. Dishes containing normal, dysgenic, and transfected myotubes were fixed, freeze-fractured, and replicated for electron microscopy. Numerous small domains in the surface membrane of normal myotubes contain ordered arrays of intramembrane particles in groups of four (tetrads). The disposition of tetrads in the arrays is consistent with alternate positioning of tetrads relative to the underlying feet of the sarcoplasmic reticulum. Dysgenic myotubes have no arrays of tetrads. Some myotubes from successfully transfected cultures have arrays of tetrads with spacings equal to those found in normal myotubes. Thus the dihydropyridine receptor appears to be needed for the formation of tetrads and their association with the sarcoplasmic reticulum feet. This result is consistent with the hypothesis that each tetrad is composed of four dihydropyridine receptors.

INTRODUCTION

Excitation contraction (e-c) coupling is initiated by depolarization of the surface membrane and transverse (T) tubules followed by the release of calcium from the sarcoplasmic reticulum (SR). In skeletal muscle the junctions between SR and T tubules (triads and dyads) and between SR and surface membrane (peripheral couplings) have two major components. The junctional domain of the SR is occupied by feet (Franzini-Armstrong, 1970; Block et al., 1988), constituting the calcium release channels (Lai et al., 1988). The junctional domains of the external surface membrane and of T tubules are occupied by arrays of tetrads, each of which is composed of four intramembranous particles (Franzini-Armstrong and Nunzi, 1983; Franzini-Armstrong, 1984; Block et al., 1988; Franzini-Armstrong et al., 1991; Takekura and Franzini-Armstrong, 1994). The precise relationship between the disposition and spacing of tetrads in the junctional domains of T tubules and of feet in the SR suggests that the two sets of proteins are directly or indirectly linked.

Dihydropyridine receptors (DHPRs), which have been proposed to be the voltage sensors of e-c coupling (Rios and Brum, 1987), are located in the T tubules of adult skeletal muscle (Fosset et al., 1983; Jorgensen et al., 1989; Flucher et al., 1990) and in the surface membrane of developing muscle (Yuan et al., 1991). The gene encoding the DHPR of skeletal muscle is altered in mice with the muscular dysgenesis (*mdg*) mutation (Tanabe et al., 1988; Chaudari, 1992). As a result, skeletal muscle cells from homozygous mdg/mdg mice lack DHPRs (Knudson et al., 1989), e-c coupling and slow calcium currents (Beam et al., 1986), and immobilization-resistant charge movement (Adams et al., 1990). Transfection of cultured dysgenic muscle cells with cDNA encoding skeletal muscle DHPR restores e-c coupling, slow calcium current (Tanabe et al., 1988), and immobilization-resistant charge movement (Adams et al., 1990), supporting the idea that DHPRs function as slow calcium channels and as voltage sensors for e-c coupling.

It has been proposed that each tetrad is composed of four DHPRs located in a position that allows their interaction with the four subunits of a foot (Block et al., 1988). Consistent with this hypothesis, DHPRs, like tetrads, are located in the junctional domains of T tubules and surface membrane (Flucher et al., 1990; Jorgensen et al., 1989; Yuan et al., 1991). Furthermore, tetrads are absent from the surface membrane of developing muscle fibers from dysgenic mice (Franzini-Armstrong et al., 1991).

Here, we have analyzed cultured muscle fibers as a means of testing the hypothesis that junctional tetrads represent assemblies of DHPRs. We report that, as in muscle fibers developing in vivo, tetrads are present in primary muscle cultures from normal mice but absent in cultured muscle from dysgenic mice. Moreover, transfection of cultured, dysgenic muscle cells with cDNA encoding the skeletal DHPR causes the reappearance of tetrads in appropriately spaced arrays, indicating a direct relationship between tetrads and DHPRs. A preliminary report of this work has been presented (Takekura et al., 1993).

Received for publication 23 February 1994 and in final form 25 May 1994.

Address reprint requests to Dr. Clara Franzini-Armstrong, Department of Cell and Developmental Biology, University of Pennsylvania School of Medicine, Philadelphia, PA 19104-6058. Tel.: 215-898-3345; Fax: 215-573-2170.

0006-3495/94/08/793/11 $2.00

MATERIALS AND METHODS

Primary cultures of myotubes were prepared by harvesting limb and trunk muscles from newborn mouse pups that were either homozygous (mdg/mdg) for the muscular dysgenesis mutation (Pai, 1965) or phenotypically normal (+/mdg?). The muscles were incubated for 30–60 min at 37°C in calcium/magnesium-free Ringer's (155.5 mM NaCl, 5 mM KCl, 11 mM glucose, 10 mM HEPES, pH 7.4 with NaOH) containing (w/v) 0.25% crude trypsin (1:250, Difco Laboratories Inc., Detroit, MI). Trituration and centrifugation were used to obtain mononucleated cells, which were plated in (v/v) 85% Dulbecco's modified Eagle's medium with 4.5 g/l glucose (DMEM) and 15% fetal bovine serum at 2×10^5 cells/dish into 35-mm plastic dishes which either contained an attached layer of fibroblasts (Adams and Beam, 1989) or had been coated with 10% gelatin. After 24 h, the plating medium was replaced with maintenance medium (90% DMEM, 10% horse serum). All media contained penicillin (100 U/ml) and streptomycin (100 μg/ml).

Two to three hours after the change from plating to maintenance medium, calcium phosphate-mediated DNA transfer (Chen and Okayama, 1988) was used to transfect dysgenic cells with pCAC6, an expression plasmid encoding the full-length rabbit skeletal DHPR (Tanabe et al., 1987, 1988). The cells were exposed for 24 h to "transfection solution," prepared by vortexing one volume each of 250 mM $CaCl_2$ and 2X PIPES saline (280 mM NaCl, 50 mM PIPES, 1.5 mM Na_2HPO_4, pH 6.95) with the plasmid DNA (final DNA concentration of 0.1 mg/ml). Afterward the cells were returned to maintenance medium.

Seven days after original plating, dishes containing transfected dysgenic myotubes were systematically scanned to determine the percentage of myotubes that contracted in response to electrical stimulation (Tanabe et al., 1988). Although not routinely monitored, the percentage of contracting myotubes in normal cultures was typically 40–60%. No contractions were observed in non-transfected dysgenic cultures. The percentage of contracting myotubes in transfected cultures varied between 0 and 40%, and only those dishes that displayed a minimum of 20% contracting myotubes were fixed for electron microscopy. Quantitative data were obtained from a culture on which 40% of the myotubes were rescued and the content of fibroblasts was low. For fixation, the dishes were rinsed with phosphate-buffered saline (134.34 mM NaCl, 4.36 mM KCl, 10.56 Na_2HPO_4, 1.66 mM NaH_2PO_4, pH 7.4) and then exposed at room temperature to a solution containing (v/v) 50% phosphate-buffered saline and 50% fix solution (3% glutaraldehyde in 0.1 M Na-cacodylate buffer, pH 7.4). After 10 min, this solution was removed and 100% fix solution was added to fill the dishes, which were sealed with parafilm. The fixed cultures were kept for up to several weeks at 4°C, with an interval of about 2 days at room temperature for shipping between laboratories.

For freeze-fracture, the cultures were cryoprotected in 30% glycerol, 20% DMSO, and a small section of the culture was gently lifted from the dish and its free (formerly top) surface adhered to a piece of glass coverslip coated with 0.2% gelatin. The coverslip was then inverted on a gold holder covered with a droplet of 15% polyvinyl alcohol in 30% glycerol and the sandwich was frozen in either Freon or propane and fractured in the double replica holder of Balzer's 400 freeze-fracture apparatus (Pauli et al., 1977; Cohen and Pumplin, 1979; Osame et al., 1981). The gold side of the replica was cleaned in Clorox and examined in a Philips 400 electron microscope.

RESULTS

General description

The studies described here were carried out on small sections (1–4 mm^2) of muscle cultures that were freed from the culture dish and adhered, via their free surface, to glass slides. Because the fracture plane tended to follow the surface of cells that faced the glass slide, the cytoplasmic leaflet of myotube, the region of interest in this study, was located on the side of the double replica that remained associated with the gold holder. The cultures used in this study had well developed myotubes, mixed with other cells, probably fibroblasts and myoblasts. Cytoplasmic leaflets of myotubes are easily distinguishable from those of the other cells, because the myotubes have more numerous intramembranous particles and because the cells have a fusiform or approximately cylindrical shape. Fractured profiles of short segments of myotubes are usually interspersed between extended profiles of other cells. Occasionally a single myotube can be followed over several grid squares.

Normal myotubes; arrays of tetrads

Normal cultured mouse myotubes have three obvious surface specializations: openings of caveolae, small groups of particles of variable size and spacings, and groups of tetrads. The latter are illustrated at low magnification in Fig. 1 *A*, where groups of tetrad are located immediately above curved lines. Tetrads occupy membrane domains from which other particles of assorted size are excluded and form part of ordered arrays (see below). Often, but not always, the domains sit on a slightly domed patch of membrane. At higher magnification (Fig. 1 *B*) individual tetrads (*circles*) are clearly identified, but the arrays seem incomplete because most of the tetrads have some missing elements due to distortion during fracturing.

The groups of tetrads in cultured mouse myotubes differ in two respects from those found in myotubes developing in vivo (Franzini-Armstrong, 1991). First, the groups are distributed quite unevenly along the cultured myotubes: long (up to hundreds of microns) stretches of myotubes without any tetrads (not shown) alternate with segments in which tetrads are very numerous (Fig. 1 *A*). In three randomly selected fractures from normal cultures, we counted a total of 94 myotube segments, and of these 24 (26%) had numerous groups of tetrads in them, the others had none (Table 1). A second difference between myotubes developing in vivo and in vitro is that in the latter the groups of tetrads are quite variable in size and some of them are very large.

Transfected and non-transfected dysgenic myotubes

In transfected myotubes, groups of tetrads are present (Fig. 2 *A*), but the groups are less frequent and contain fewer tetrads than in normal myotubes. An initial survey at the microscope of a transfected culture with 40% rescued (contracting) myotubes showed that of a total of 105 myotube segments in 14 freeze-fractures, 8 (7.6%) contained groups of tetrads (Table 1). Within each group, some tetrads are well preserved (Fig. 2 *B*, *circles*) and others are distorted in fracturing, just as in normal myotubes. In cultures with very low (10%) level of rescue, we found rare, very small groups of tetrads.

In dysgenic myotubes all segments are equal: none show groups of tetrads (Fig. 2 *C*). Examination in the microscope of 85 segments in 7 freeze-fractures failed to show segments containing one or more obvious groups of tetrads (Table 1). Some groups of particles, which are found in normal, dysgenic, and transfected myotubes, clearly differ from groups of tetrads (compare Fig. 2 *B* and 2 *D*).

Individual, well preserved tetrads in normal (Fig. 3, *A* and *B*) and transfected (Fig. 3, *C–F*) myotubes are of the same size and are formed by four equal components. In each group of tetrads found in normal and transfected myotubes,

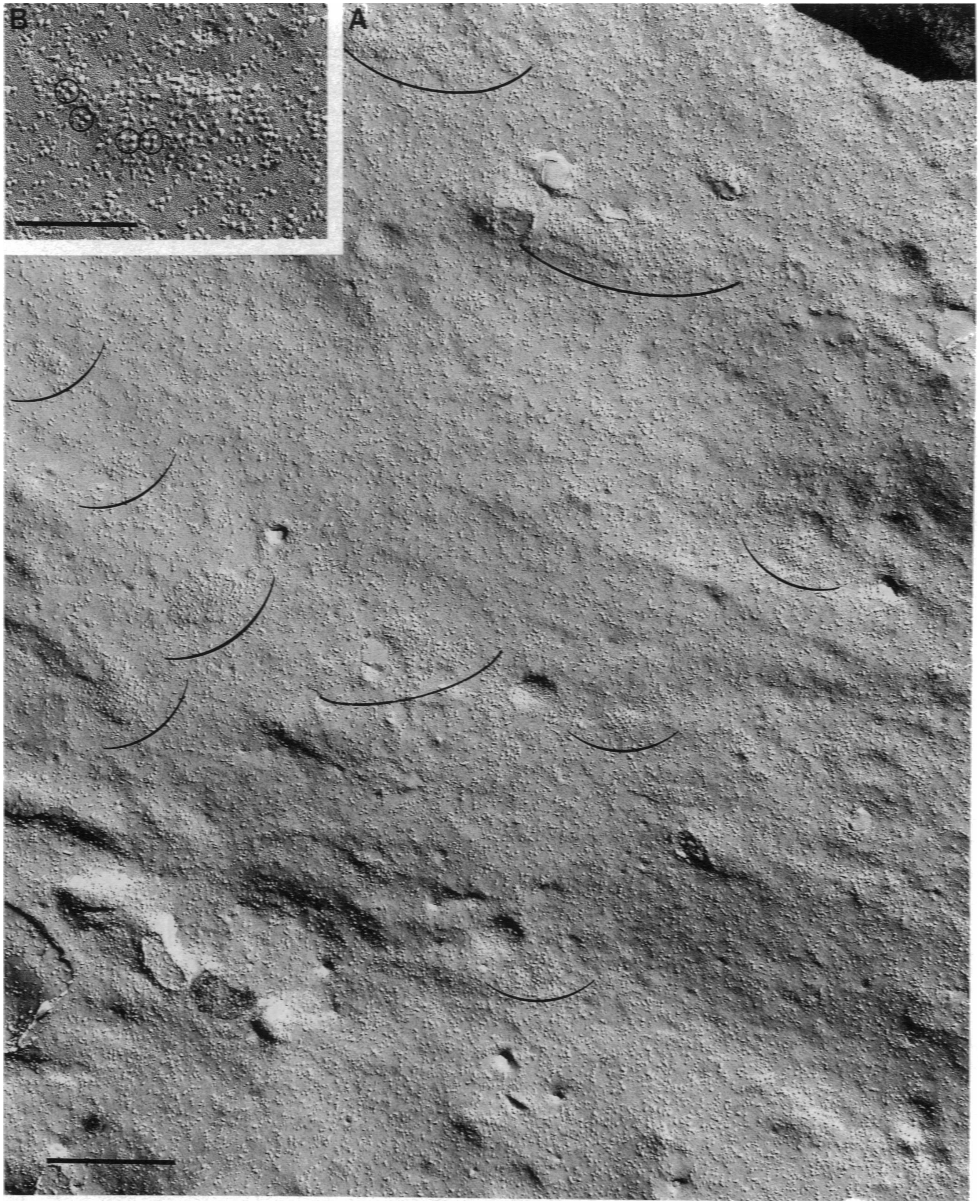

FIGURE 1 (*A*) Freeze-fracture through the surface membrane of a myotube in a primary culture of normal mouse skeletal muscle, illustrating a patch of membrane rich in groups of tetrads (*semicircles*). At this low magnification the groups are recognizable, because the membrane domain occupied by tetrads is slightly domed and the tetrads are formed by large particles. The sizes of the groups are variable. ×93,000; scale bar = 0.25 μm. (*B*) Detail of a group of tetrads. Complete tetrads (*circles*) are formed by four symmetrically arranged, equal-sized particles. Note that most tetrads in this group either miss some components or show some distortion due to the fracturing process. ×226,000; scale bar = 0.1 μm.

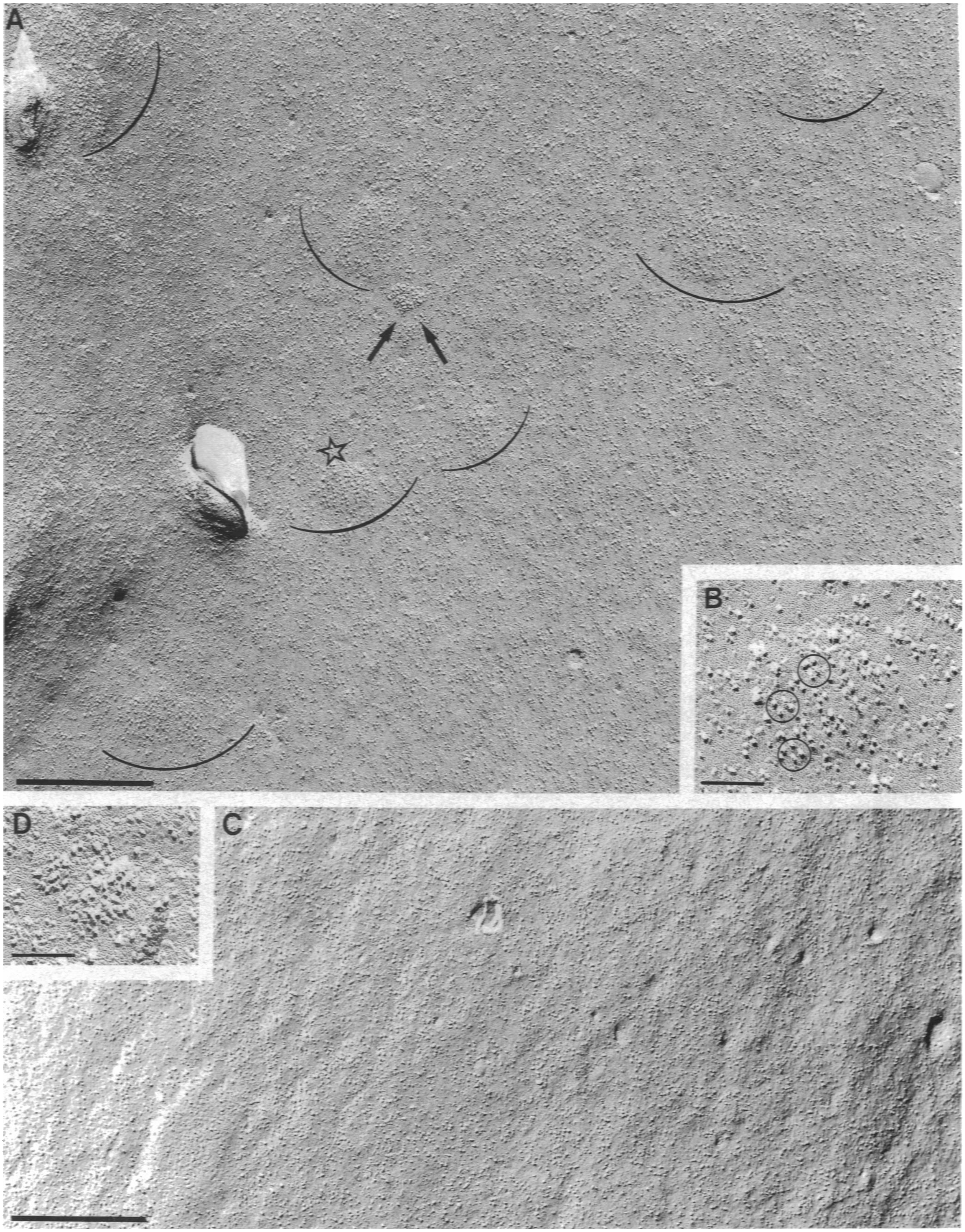
A
B
D
C

TABLE 1 Measured parameters of normal, dysgenic, and transfected cultured mouse muscle fibers

Muscle	No. of myotube segments	Myotube segments with tetrads[*]	Groups of Particles[‡]				Spacings Between Tetrads[§]		
			Total	Pos. %	Neg. %	Null %	Long spaces[¶] (nm)	Short spaces[‖] (nm)	Ratio L/S
Control	94	26	184	67	18	15	54.7 ± .34 (235)	38.7 ± .26 (216)	1.41
Dysgenic	85	0	80	0	82	18			
Transfected	105	8	230	65	23	12	53.2 ± .34 (180)	37.7 ± .24 (197)	1.41

[*] Myotube segments in which tetrads were initially identified at the electron microscope.
[‡] Groups of closely arranged large particles. Of these, some are identifiable as groups of tetrads (positive), others do not fulfill the criteria for the identification given in the text (negative) and others clearly are quite different from groups of tetrads (null).
[§] Data are given as mean ± SEM, with number of measurements in parenthesis. Each measurement is the average of the distance between 2–5 aligned tetrads.
[¶] Spacings between tetrads in the direction of the arrows (Figs. 5 and 6).
[‖] Spacings between tetrads in the direction of the dotted lines. (Figs. 5 and 6).

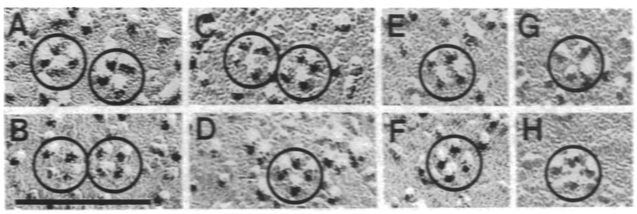

FIGURE 3 Individual tetrads in normal (*A* and *B*) and in transfected myotubes (*C–F*) have similar appearance. The size of the individual particles forming a tetrad varies somewhat depending on the amount and angle of the platinum shadow, but within each well-preserved tetrad the four particles are symmetrically disposed to form a square. (*G–H*) four particles grouped to form an apparent tetrad are occasionally visible in the membrane of dysgenic myotubes. However, these groups of four particles are irregular in shape and are not parts of an array (see also Figs. 4 and 5). ×227,000; scale bar = 0.1 μm.

at least one well preserved tetrad is visible. In areas of normal and transfected myotubes in which groups of tetrads are absent and also in non-transfected dysgenic myotubes, the numerous intramembrane particles do occasionally aggregate into groups of four, as illustrated in Fig. 3, *G* and *H* (dysgenic myotubes). These random "groups of four," however, differ from tetrads because the four components are not of equal size, and, more importantly, because they are not grouped in special membrane domains, as shown in Fig. 4. Fig. 4 compares groups of tetrads in normal (*A*) and transfected (*C* and *D*) cells. Each group of tetrads occupies a membrane domain in which several tetrads (*circles*) are well recognizable and large particles belonging to incompletely visible tetrads complete the array. By contrast, in dysgenic myotubes (Fig. 4 *B*), there are only "apparent tetrads" (*circles*), and these are separated from each other by regions containing very few large particles.

To confirm the initial identification of groups of tetrads we designed a blind test for the absence or presence of tetrads. Unlabeled micrographs were given to two sets of physiologists (K. G. B. and L. B. formed one group, and Dr. Steve Baylor, University of Pennsylvania the other) along with some criteria for detecting the groups of tetrads: the presence of at least one complete tetrad, and slight outward bulging of the membrane. K. G. B. and L. B. performed the test in the most stringent manner: they accepted as tetrads only the best preserved examples in which four identical looking particles are present. Dr. Baylor relied on a wider range of clues, including the fact that tetrads are grouped and thus they can be recognized even when some of the components are missing and the fact that usually several groups of tetrads are present in each image, and thus finding more than one reinforces the identification.

Of the 102 test pictures, 11 were from normal cultures, 67 from transfected fibers, and 24 from non-transfected dysgenic cultures. The two electron microscopists in the group (H. T. and C. F. A.) had identified groups of tetrads in all the micrographs from normal and transfected cells and none in the images from dysgenic fibers. K. G. B. and L. B. identified groups of tetrads in 82% of the normal and 68% of the transfected images. They identified one dysgenic image as containing tetrads, so that on 96% of the dysgenic images they agreed with the electron microscopist that tetrads were not present. Dr. Baylor agreed in the identification of 100% of normal and 89% of transfected images, and his agreement with the microscopists on the dysgenic ones was 88%, i.e., he detected possible groups of tetrads in three images from dysgenic fibers. Thus on the basis of a simple visual inspection, the large groups of tetrads on the surface of normal fibers are readily identifiable, the smaller and less frequent

FIGURE 2 (*A*) Fracture through the surface membrane of a myotube from a dysgenic culture which was transfected with cDNA for the DHPR. In this culture 40% of the myotubes contracted in response to stimuli. This patch of membrane has many small groups of tetrads (*semicircles*) occupying slightly domed membrane domains. The group of tetrads marked by an asterisk is shown in detail in *B*. Arrow points to a group of tightly arranged particles different from the groups of tetrads (see also *D*). ×48,000; scale bar = 0.5 μm. (*B*) Detail of a group of tetrads in a rescued myotube. Complete tetrads are circled; others miss some components. ×119,000; scale bar = 0.1 μm. (*C*) Fracture through the surface membrane of a myotube from a non-transfected dysgenic culture. In dysgenic myotubes groups of tetrads are not seen and the surface membrane has a uniform appearance, as shown here. ×48,000; scale bar = 0.5 μm. (*D*) Detail of a group of tightly arranged particles from a dysgenic myotube. Such groups are occasionally found in all types of myotubes (normal, dysgenic, and transfected, see *A*). They are clearly distinct from groups of tetrads. ×119,000; scale bar = 0.1 μm.

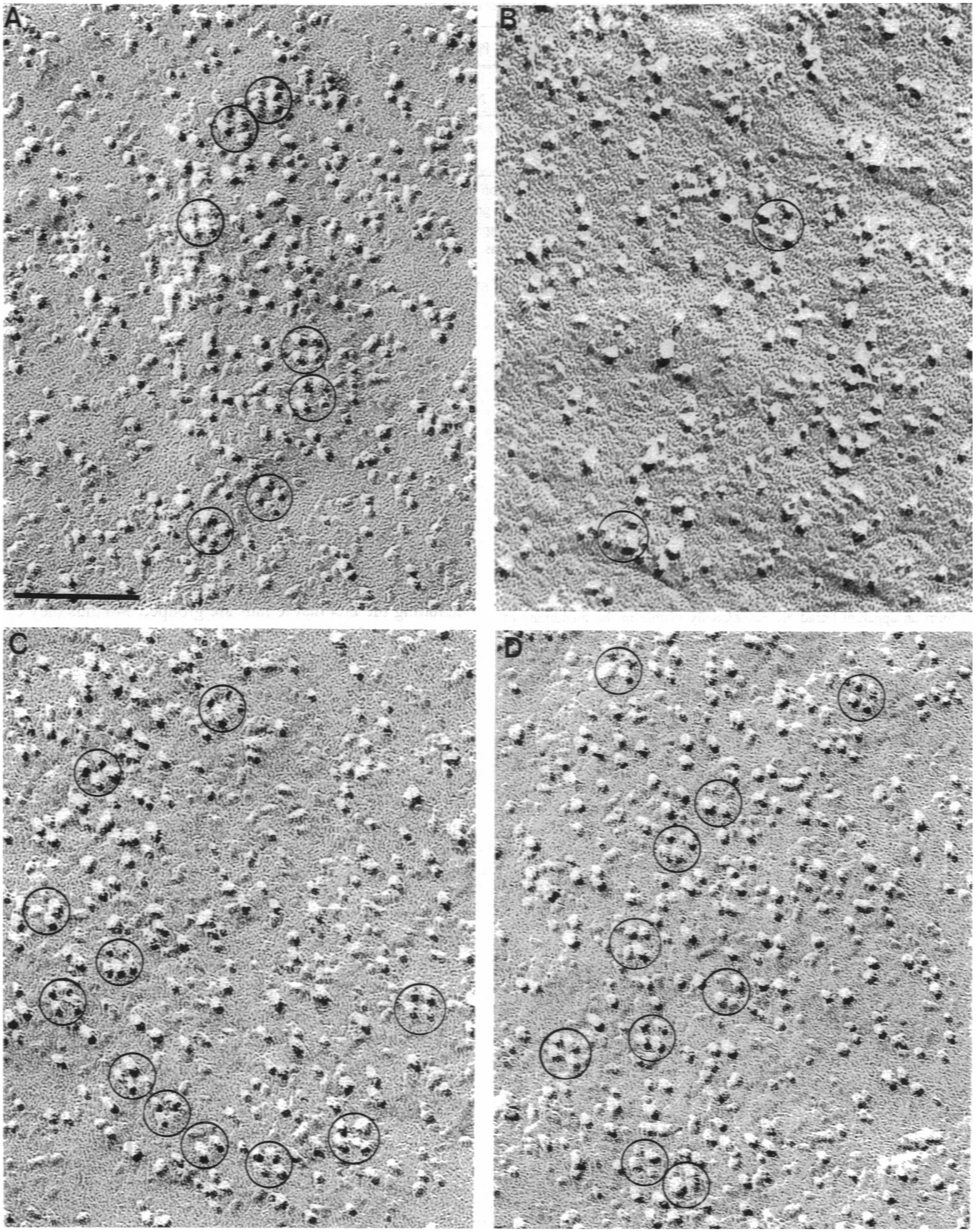

FIGURE 4 Large groups (arrays) of tetrads are observed in the surface membrane of normal (*A*) and transfected (*C, D*) dysgenic myotubes but not in control dysgenic (*B*) myotubes. Note that in *A, C*, and *D* several well identifiable tetrads are present in each array (*circles*), that within the array large particles occupy the gaps between the well identifiable tetrads, and that in many instances these large particles can be recognized as forming incomplete or distorted tetrads. In dysgenic myotube (*B*) random assemblages of four particles are occasionally observed (*circles*), but these do not have the regular structure of tetrads and do not form part of an array of large particles. ×227,000; scale bar = 0.1 μm.

groups of tetrads on transfected fibers are identifiable with a fairly high level of confidence, and some questions are raised on whether dysgenic fibers are devoid of groups of tetrads.

A more stringent test for identification is based on the observation that tetrads form precise arrays, as seen in the peripheral couplings of embryonal mouse skeletal muscle in vivo (Fig. 5 *A*). Within each group of tetrads a tetragonal array of dots defines the centers of the tetrads. Once a dot is placed in the center of each complete and/or incomplete tetrad in the array, the grouping and alignment of tetrads is quite clear and is emphasized by the fact that narrow strips of smooth membrane separate the lines of tetrads (Fig. 5 *A'*). Four directions are defined within the array: two along which the tetrads are contiguous with each other (Fig. 5 *A'*, *dotted lines*), the other two along which tetrads alternate with empty spaces (Fig. 5 *A'*, *arrow*). In each array the tetrads line up with their diagonal axes slightly tilted relative to the two main directions along which the tetrads are aligned in close proximity to each other.

With the above information in mind, micrographs collected from normal and transfected myotube segments containing presumed groups of tetrads and micrographs collected from areas of dysgenic fibers that contained groups of particles differing from complete randomness were examined as follows. First each group of particles was overlaid with dots centered on groupings that might represent tetrads in the manner shown in Fig. 5, *A* and *A'*. Second, each group of particles was classified as follows: positive, if it contained at least four (complete or partial) tetrads at the corner of a rhombus, or five (complete or partial) tetrads with even spacing along a straight line; negative, if it contained some (complete or partial) tetrads, but not this minimum grouping; null, if it had groups of particles clearly distinct from tetrads. Fig. 5 *B–B'* to *D–D'* and 5 *E–E'* to *H–H'* show examples of positive groups in normal and transfected myotubes, respectively. Note that the components of the tetrads cluster around each dot, leaving narrow smooth strips of membrane between them.

In normal fibers we examined a total of 184 groups of particles from 62 micrographs (from four freeze-fractures, three cultures). 123 (67%) of the groups of particles were positive, 33 (18%) were negative, and 28 (15%) were null (Table 1). In transfected fibers we examined 230 groups from 53 micrographs (from four freeze-fractures, two dishes of the same culture): these comprise all the micrographs from areas in which groups of tetrads were tentatively identified while examining the fractures in the electron microscope. 149 (65%) of these groups were positive, 53(23%) were negative, and 28 (12%) were null (Table 1). In dysgenic fibers we examined 58 micrographs (from four freeze-fractures, two cultures) taken from areas where examination in the electron microscope revealed some grouping of particles. In these micrographs we found 80 groups of particles, of which 0 (0%) were positive, 66 (82%) were negative, and 14 (18%) were null (Table 1). The relatively large number of null groups in dysgenic fibers is due to one micrograph that had numerous groups of particles of the type shown in Fig. 2 *D* within a small area. Thus based on this more stringent set of criteria, groups of tetrads are present in normal and transfected dysgenic but not in non-transfected dysgenic myotubes. Fig. 4 *B* shows an image from a dysgenic myotube that in the blind test described above had been tentatively identified to contain some tetrads. It is clear that this image would be considered negative on the basis of the more stringent criteria.

Finally, within groups of tetrads from normal and transfected myotubes, we measured the distance between dots marking the apparent centers of tetrads, along the two directions described above and indicate by dotted lines and arrows in Fig. 5, *B'* to *H'*. This gives long (along the arrow) and short (along the dotted line) center-to-center distances between aligned tetrads. In 39 groups of tetrads in normal fibers the average long and short distances between tetrads are 54.7 ± 0.34 and 38.7 ± 0.26 nm (mean ± 1 SEM), respectively (Table 1). In 42 groups from transfected fibers the means for long and short distances are 53.2 ± 0.34 and 37.7 ± 0.24 (Table 1). The ~3% difference in spacing between control and transfected fibers may in part be accounted for by the fact that in normal fibers the arrays of tetrads are more extensive and thus the distances are less affected by tilt of the membrane at the edges of the domed patches on which the arrays reside.

We analyzed the disposition of tetrads in control and transfected fibers as follows. First we constructed an extended array of feet based on the expectation that their disposition is the same as in triads of vertebrates. Feet are formed by four equal subunits, represented by spheres, and they are located so that one subunit from a foot overlaps with that of a neighbor and a line drawn through two adjacent subunits of one foot runs through two subunits of the adjacent foot (Fig. 6 *A*). This is the configuration that has been directly observed in shadowed images of SR from skeletal muscle of rat, guinea pig, and frog (Ferguson et al., 1984) and which produces the best fit between the known structure of feet and images of grazing views of arrays of feet in thin section from frog (Franzini-Armstrong, 1984), fish (Franzini-Armstrong, 1975; Block et al., 1988), rabbit (Mitchell et al., 1983), and Amphioxus (C. Franzini-Armstrong, unpublished observations). Note that the center of the feet are on an orthogonal lattice, but the feet show a tilted offset relative to lines connecting their centers. This quite precisely mimics the actual images. Second, we constructed an array in which tetrads occupy the position of alternate feet (Fig. 6 *B*). Feet on which tetrads are centered are indicated by central dots in Fig. 6 *A*. The overall size of each tetrad in Fig. 6 corresponds approximately to that in actual micrographs (see Fig. 5 *A*) and thus is slightly larger than that of the feet in Fig. 6 *A*. This is not necessarily due to a larger size of the four proteins comprising the tetrads relative to the feet subunits (as implied by the drawing), but it may simply be due to a slight offset in the position of the four components of the tetrads relative to the four subunits of the feet. The size of the tetrads does not affect their center-to-center distance. Arrows and dotted

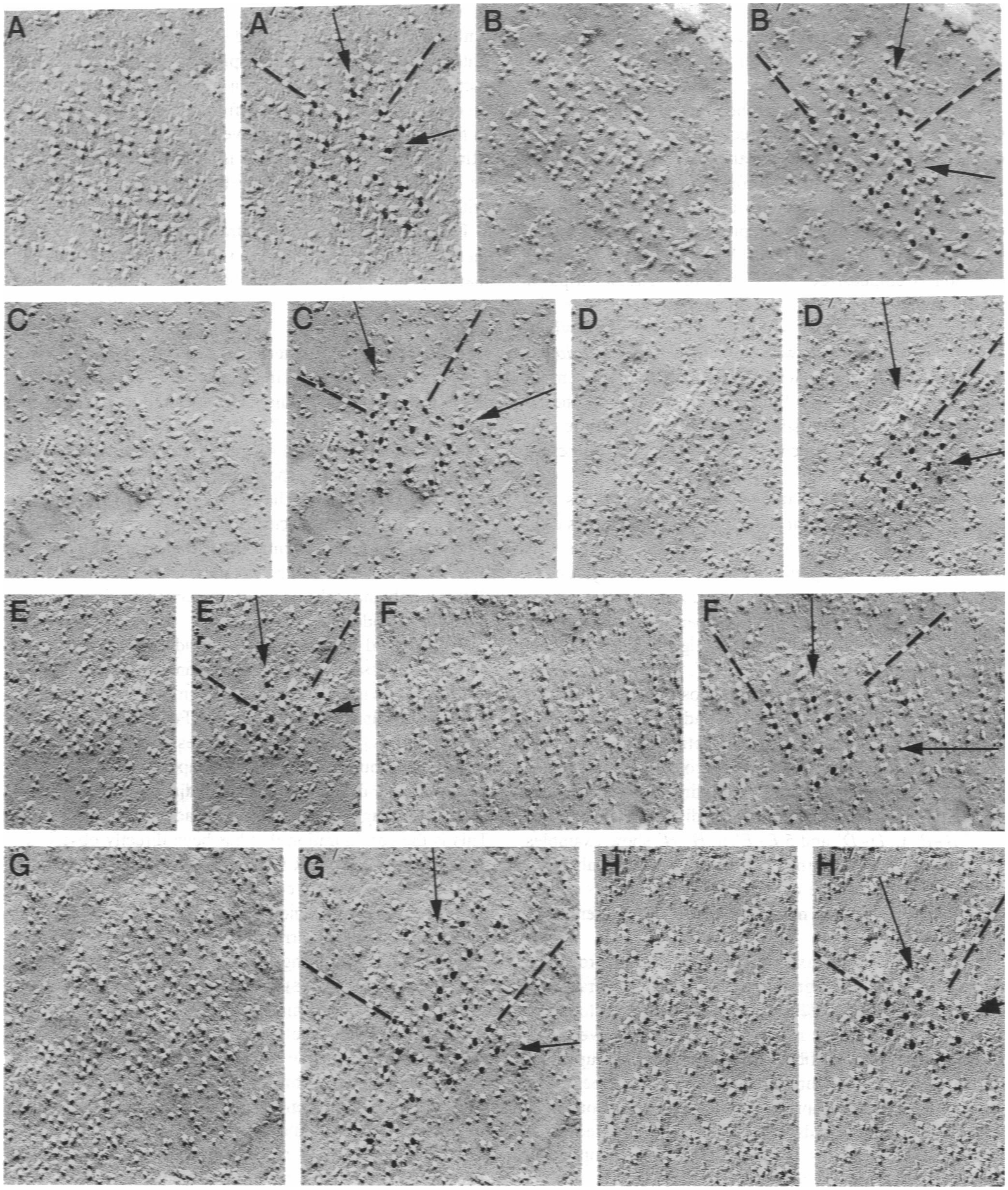

FIGURE 5 Arrays of tetrads in myotubes from a normal in vivo mouse embryo (*A, A'*), normal primary cultures (*B, B'* to *D, D'*), and transfected dysgenic myotubes (*E, E'* to *H, H'*). Non-transfected dysgenic myotubes do not show such arrays. Each micrograph is shown unaltered (*left*) and with the addition of dots to mark the centers of tetrads (*right*). The dots help to visualize the arrays and reveal the presence of clear strips of smooth membrane between the lines of tetrads. Four directions are recognized in the arrays; along two directions (*dotted lines*) the tetrads are in close proximity to each other. Along the other two directions (*arrows*), tetrads alternate with empty spaces of a size approximately equal to that of the tetrads. (Holding the photographs at eye level and sighting along the dotted lines helps to visualize the underlying order.) Note that the alignment of tetrads is better preserved in the in vivo than in the in vitro case. This is due to the fact that the cultured cells were sandwiched between a glass slide and a gold holder for freezing and thus the cooling was fairly slow. Minor ice damage is responsible for some disorder in the images. ×105,000–118,000; scale bar = 0.1 μm.

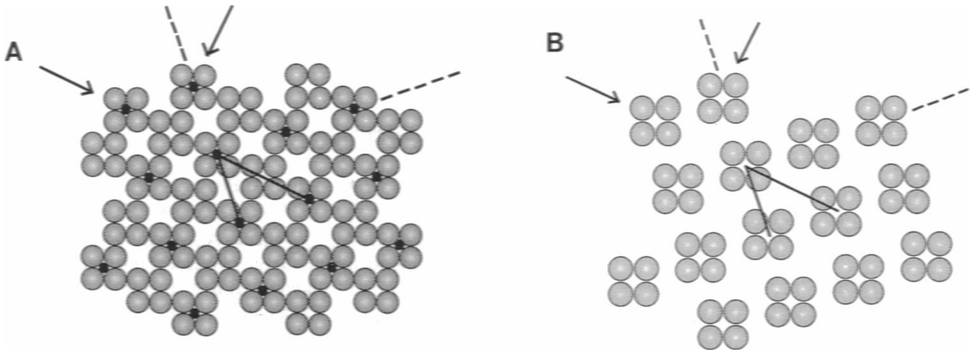

FIGURE 6 Geometric arrangement of feet and tetrads. (*A*) Extended array of feet constructed following the guidelines in Ferguson et al., 1984 (see also text). Alternate feet are marked by a central dot. In the direction of the arrows, dotted feet alternate with unmarked ones. This is the direction equivalent to that parallel to the long axis of transverse tubules in triads. The spacing between dotted feet in this direction (long spacing) is the hypotenuse of a right triangle, whose sides are 2 and 4 times the diameter (a) of one of the foot subunits. The spacing between feet in the direction of the dotted lines is the hypotenuse of a right triangle with sides $1a$ and $3a$. Given a foot that is 26 nm on its side (a = 13 nm), the two spacings are 58 and 41 nm, respectively. (*B*) Array of tetrads built by centering the tetrads above the dotted feet of *A*. The arrows and dotted lines correspond to the two directions indicated by the same symbols in Fig. 5, *A–H*. The long and short distances between tetrads are the same as those between dotted feet in *A*.

lines in Fig. 6, *A* and *B*, indicate the two directions along which measurements of long and short center-to-center distances between tetrads were taken in the electron micrographs of control and transfected fibers (compare with Fig. 5, *A′–H′*). The long and short spacings are indicated by two continuous lines joining alternate (dotted) feet in Fig. 6 *A* and adjacent tetrads in Fig. 6 *B*. Simple geometric considerations, based on Fig. 6 *A*, indicate that the center-to-center distance between dotted feet in the direction of the arrow (long distance) is $D = a\sqrt{20}$, where a is the diameter of a foot subunit, while the distance in the direction of the dotted lines (short distance) is $d = a\sqrt{10}$. The side of the foot protein has been most accurately measured to be 26 nm in negatively stained images (Lai et al., 1988) and this has been subsequently confirmed (Saito et al., 1988; Wagenknecht et al., 1989). Based on that measurement, the subunit diameter (a) is 13 nm, and the predicted long and short distances between alternate (dotted) feet are 58 and 41 nm. The calculated ratio of long and short distances in Fig. 6, *A* and *B* is $\sqrt{2}=1.41$. These numbers agree very well with measurements in toadfish muscle, where the average center to center distance between tetrads along the length of T tubules, which corresponds to the direction of the arrows in Fig. 6, *A* and *B*, is 58 nm and the distance between feet in the same direction is 28 nm (Block et al., 1988).

There are two points of perfect convergence between the model of Fig. 6 *B* and the micrographs of groups of tetrads in this study: 1) the disposition of tetrads is the same: in one direction the tetrads alternate with empty spaces, in another they are more closely disposed; 2) the ratios of the long and short distances in groups of tetrads from control and transfected fibers is 1.41, i.e., equal to the ratio predicted by the model (see above).

A small (6–8%) discrepancy is, however, apparent between the model and the data in the actual spacings of tetrads and feet. The long center-to-center distance between tetrads predicted from Fig. 6, *A* and *B*, based on the known foot size for rabbit muscle (see above) is 58 nm, while the measured long distances in our micrographs are 53.2 and 54.7 nm for normal and transfected myotubes, respectively. One possibility is that the spacing between feet in mouse is slightly smaller than predicted from the model of Fig. 6 *A*, based on a foot size of 26 nm. Indeed, the model predicts a center-to-center distance between adjacent feet of 29.1 nm, whereas the actual spacing observed in adult mouse EDL muscle is 26.1 ± 1.2 nm (mean ± 1 SD, from 459 spacings in 30 triads). This fits well with the measured distances between tetrads, if the tetrads are associated with alternate feet. If tetrads were arrayed in a 1:1 ratio to feet, a possibility that was previously considered (Franzini-Armstrong et al., 1991), then the spacing between tetrads would be equivalent to the center-to-center distance between ryanodine receptors, which is clearly not the case.

DISCUSSION

Our results indicate that tetrads are absent from cultured dysgenic muscle fibers and reappear after transfection with the cDNA for the missing α_1 subunit of the DHPR. The most direct explanation of this finding is that tetrads are composed of DHPRs. If this is correct, then junctional tetrads are the first voltage gated ion channels to be visualized after expression of cDNA. If tetrads are not composed of DHPRs, it seems necessary to conclude that DHPRs are required for the association of four identical proteins of the surface membrane/T tubules into tetrads.

Importantly, we find that in normal and transfected fibers the tetrads are never single, but instead they are arranged in arrays with disposition and spacings related to those expected from a specific association with arrays of feet. Feet are present in dysgenic muscle in vivo (Franzini-Armstrong et al., 1991) and are well visible in dysgenic muscle in vitro after expression of DHPR (Seigneurin-Venin et al., 1994). In addition, arrays of tetrads are disposed over slightly domed patches of membrane, presumably due to the presence of an SR cisterna closely associated with the surface membrane.

The ordered arrangement of tetrads indicates that they are located in membrane domains associated with arrays of feet, i.e., they form part of peripheral couplings between SR and the surface membrane. Since tetrads appear only in the presence of DHPRs, and tetrads are associated with feet, this also indicates that DHPRs have some association with feet, whether or not DHPRs are components of tetrads (see above).

Our observations that tetrads occur in groups is consistent with immunohistological analyses of DPHR distribution. In dysgenic myotubes the α_2 subunit of the DHPR is dispersed, whereas in dysgenic myotubes functionally rescued by fusion with normal non-muscle cells (probably fibroblasts), both the α_1 and α_2 subunits are clustered in hot spots (Flucher et al., 1991). In addition, peripheral couplings are relatively frequent in normal myotubes, but rare and not well developed in dysgenic ones (Pincon-Raymond et al., 1985). A correlation between presence of tetrads in the surface membrane and peripheral couplings has also been established in developing muscle and in frog slow fibers (Franzini-Armstrong, 1984; Franzini-Armstrong et al., 1991; Takekura et al., 1994).

Dispositions and spacings of tetrads in control and transfected myotubes correlate excellently with those predicted from an array in which tetrads are disposed in correspondence to alternate feet (see Results). In a previous publication (Franzini-Armstrong et al., 1991), it was noted that grouped tetrads in the surface membrane of embryonal mouse muscle are fairly closely spaced in one direction and on that basis a 1:1 relationship between tetrads and feet was proposed, while noting, however, that the measured spacing was not entirely consistent with that hypothesis. The more complete analysis performed here predicts a tetrad-to-feet ratio of 1:2, as previously found in T-SR junctions of fish muscles (Franzini-Armstrong and Nunzi, 1983; Block et al., 1988). If tetrads are composed of four DHPRs, this would predict a 2:1 ratio for DHPR/RyR. However, ligand binding data have given variable results. While some studies agree with a 2:1 ratio (Bers and Stiffel, 1993; Lamb, 1992), others find lower and different ratios in different species (Cohn et al., 1993), and even within triad fractions from the same source (Kim et al., 1990). At the moment the structural information on the muscles used for binding studies is too incomplete to allow for a choice between various possibilities: 1) tetrad to feet ratios vary in different muscles and/or triads and this explains the binding data; 2) non-junctional feet (Dulhunty et al., 1992) and/or other molecules with high affinity for ryanodine are present; 3) tetrads are not composed of DHPRs. In this latter case, however, one must assume that the presence of DHPRs is needed for locating tetrads in precise correspondence to feet (see above).

We thank Dr. D. W. Pumplin's laboratory and Dr. A. G. Engel for sharing with us their experience with the technique for fracturing cultured cells. Nosta Glaser is commended for her infinite patience in preparing small pieces of glass coverslips and for help with the illustrations; John W. Kish for measuring spacings in hundreds of micrographs.

This work was supported by MDA and NIH HL 15835 to the Pennsylvania Muscle Institute (C. F. A.) and by NIH NS24444 and NS28323 (K. G. B.).

REFERENCES

Adams, B. A., and K. G. Beam. 1989. A novel calcium current in dysgenic skeletal muscle. *J. Gen. Physiol.* 94:429–444.

Adams, B. A., T. Tanabe, A. Mikami, S. Numa, and K. G. Beam. 1990. Intramembrane charge movement restored in dysgenic skeletal muscle by injection of dihydropyridine receptor cDNAs. *Nature.* 346:569–572.

Beam, K. G, J. M. Knudson, and J. A. Powell. 1986. A lethal mutation in mice eliminates the slow calcium current in skeletal muscle cells. *Nature.* 320:168–170.

Bers, D. M., and V. M. Stiffel. 1993. Ratio of ryanodine and dihydropyridine receptors in cardiac and skeletal muscle and implications for excitation-contraction coupling. *Am. J. Physiol.* 264:C1587–2600.

Block B. A., T. Imagawa, A. T. Leung, K. P. Campbell K. P., and C. Franzini-Armstrong. 1988. Structural evidence for direct interaction between the molecular components of the transverse tubules/sarcoplasmic reticulum junction in skeletal muscle. *J. Cell Biol.* 107:2587–2600.

Chaudari, N. 1992. A single nucleotide deletion in the skeletal muscle specific calcium channel transcript of muscular dysgenesis (mdg) mice. *J. Biol. Chem.* 267:25636–39.

Chen, C. A., and H. Okayama. 1988. Calcium phosphate-mediated gene transfer: a highly efficient transfection system for stably transforming cells with plasmid DNA. *BioTechniques.* 6:632–638.

Cohen S. A., and D. W. Pumplin. 1979. Clusters of intramembranous particles associated with binding sites for alpha-bungarotoxin in cultured chick myotubes. *J. Cell Biol.* 82:494–516.

Cohn, A. H., K. Anderson, and G. Meissner. 1993. High affinity [^{3}H]-PN200-100 and [^{3}H]ryanodine binding to rabbit and frog skeletal muscle homogenates. *Biophys. J.* 64:A152.

Dulhunty, A. F., P. R. Junankar, and C. Stanhope. 1992. Extra junctional ryanodine receptors in the terminal cisternae of mammalian skeletal muscle fibers. *Proc. R. Soc. Lond. [Biol.].* 247:69–75.

Ferguson, D. G., H. W. Schwartz, and C. Franzini-Armstrong. 1984. Subunit structure of junctional feet in triads of skeletal muscle: a freeze-drying, rotary shadowing study. *J. Cell Biol.* 99:1735–1742.

Flucher, B. E., M. E. Morton, S. C. Froehner, and M. P. Daniels. 1990. Localization of the alpha$_1$ and alpha$_2$ subunits of the dihydropyridine receptor, and ankyrin in skeletal muscle. *Neuron.* 5:339–351.

Flucher, B. E., J. L. Phillips, and J. A. Powell. 1991. Dihydropyridine receptor alpha subunits in normal and dysgenic muscle in vitro: expression of alpha$_1$ is required for proper targeting and distribution of alpha$_2$. *J. Cell Biol.* 115:1345–1356.

Fosset, M., E. Jaimovich, E. Delpont, and M. Lazdunski. 1983. [^{3}]H Nitrendipine receptors in skeletal muscle: properties and preferential location in transverse tubules. *J. Biol. Chem.* 258:6086–6092.

Franzini-Armstrong, C. 1970. Studies of the triad: I. Structure of the junction in frog twitch fibers. *J. Cell Biol.* 47: 488–499.

Franzini-Armstrong, C. 1975. Membrane particles, and transmission at the triad. *Fed. Proc.* 34:1382–1389.

Franzini-Armstrong, C. 1984. Freeze-fracture of frog slow tonic fibers. Structure of surface and internal membranes. *Tissue Cell.* 16:146–166.

Franzini-Armstrong, C., and G. Nunzi. 1983. Junctional feet and membrane particles in the triads of a fast twitch muscle fiber. *J. Muscle Res. Cell Motil.* 4:233–252.

Franzini-Armstrong, C., M. Pincon-Raymond, and F. Rieger. 1991. Muscle fibers from dysgenic mouse in vivo lack a surface component of peripheral couplings. *Dev. Biol.* 146:364–376.

Jorgensen, A. O., A, C-Y. Shen, W. Arnold, A. T. Leung, and K. P. Campbell. 1989. Subcellular distribution of the 1:4-dihydropyridine receptor in rabbit skeletal muscle in situ: an immunofluorescence and immunogold labeling study. *J. Cell Biol.* 109:135–147.

Kim, K. C., A. H. Caswell, J. P. Brunschwig, and N. R. Brandt. 1990. Identification of a new subpopulation of triad junctions isolated from skeletal muscle: morphological correlations with intact muscle. *J. Membr. Biol.* 113:221–235.

Knudson, C. M., N. Chaudari, A. H. Sharp, J. A. Powell, K. G. Beam, and K. P. Campbell. 1989. Specific absence of the alpha$_1$ subunit of the dihydropyridine receptor in mice with muscular dysgenesis. *J. Biol. Chem.* 264:1345–1348.

Lai, F. A., H. P. Erickson, E. Rousseau, Q. Y. Liu, and G. Meissner. 1988. Purification and reconstitution of the calcium release channel from skeletal muscle. *Nature.* 331:315–320.

Lamb, D. G. 1992. DHP receptors and excitation-contraction coupling. *J. Muscle Res. Cell Motil.* 13:394–405.

Mitchell, R. D. A., A. Saito, P. Palade, and S. Fleischer. 1983. Morphology of isolated triads. *J. Cell Biol.* 96:1017–1029.

Osame, M., A. G. Engel, C. J. Rebouche, and R. E. Scott. 1981. Freeze-fracture electronmicroscopic analysis of plasma membranes of cultured muscle cells in Duchenne dystrophy. *Neurology.* 31:972–979.

Pai, A. 1965. Developmental genetics of a lethal mutation (mdg) in the mouse. I. Genetic analysis and gross morphology. *Dev. Biol.* 11:89–92.

Pauli B. U., R. S. Weinstein, L. W. Soble, and J. Alroy. 1977. Freeze-fracture of monolayer cultures. *J. Cell Biol.* 72:763–769.

Pincon-Raymond, M., F. Rieger, M. Fosset, and M. Lazdunski. 1985. Abnormal transverse tubule system and abnormal amount of receptors for Ca^{2+} channel inhibitors of the dihydropyridine family in skeletal muscle from mice with embryonic muscular dysgenesis. *Dev. Biol.* 112:458–466.

Rios, E., and G. Brum. 1987. Involvement of dihydropyridine receptors in excitation-contraction coupling in skeletal muscle. *Nature.* 325:717–720.

Saito, A., M. Inui, J. Frank, and S. Fleischer. 1988. Ultrastructure of the calcium release channel of sarcoplasmic reticulum. *J. Cell Biol.* 107: 211–219.

Seigneurin-Venin, S., M. Song, M. Pincon-Raymond, F. Rieger, and L. Garcia. 1994. Restoration of normal ultrastructure after expression of the α_1 subunit of the L-type Ca^{2+} channel in dysgenic myotubes. *FEBS Lett.* 342:129–134.

Takekura, H., L. Bennett, T. Tanabe, K. G. Beam, and C. Franzini-Armstrong. 1993. Tetrads are restored in dysgenic myotubes transfected with cDNA for skeletal DHPR. *Biophys. J.* 64:A241.

Takekura, H., X-H. Sun, and C. Franzini-Armstrong 1994. Development of the excitation-contraction coupling apparatus in skeletal muscle: peripheral and internal calcium release units are formed sequentially. *J. Muscle Res. Cell Motil.* 15:102–118.

Tanabe, T., K. G. Beam, J. A. Powell, and S. Numa. 1988. Restoration of excitation-contraction coupling and slow calcium current in dysgenic muscle by dihydropyridine receptor complementary DNA. *Nature.* 336: 134–139.

Tanabe, T., H. Takeshima, A. Mikami, V. Flockerzi, H. Takahashi, K. Kangawa, M. Kojima, H. Matsuo, T. Hirose, and S. Numa. 1987. Primary structure of the receptor for calcium channel blockers from skeletal muscle. *Nature.* 328:313–318.

Wagenknecht, T., R. Grassucci, J. Frank, A. Saito, M. Inui, and S. Fleischer. 1989. Three-dimensional architecture of the calcium channel/foot structure of sarcoplasmic reticulum. *Nature.* 388:167–170.

Yuan, S., W. Arnold, and A. O. Jorgensen 1991. Biogenesis of transverse tubules and triads: immunolocalization of the 1:4-dihydropyridine receptor, TS28 and the ryanodine receptor in rabbit skeletal muscle developing in situ. *J. Cell Biol.* 110:1187–1198.